Research Article

Abdul Hadi Meteab AL Sa'adi, Fatimah Fahem Al-Khafaji, Tameem Mohammed Hashim*, Munther Latif Abdul Hussein, Yasar Ameer Ali, Alaa Hussein Ali, Yasir Mohammed Jebur, Lina H. Ali, Mohammed Zuhear Al-Mulali, and Ashraf Anwer Al-Khazraji

Prospect of using geotextile reinforcement within flexible pavement layers to reduce the effects of rutting in the middle and southern parts of Iraq

https://doi.org/10.1515/jmbm-2022-0040
received March 28, 2022; accepted May 14, 2022

Abstract: Geotextile reinforcement techniques have been widely used in paving works around the world and have proven to be effective in improving pavement performance. This study has focused on using different positions and numbers of geotextile reinforcement sheets between the layers of flexible pavement for rutting reduction. Fitting depth was measured in the field at seven constructed sections of the pavement of the road model. Each section has been strengthened with different reinforcement approaches. All road sections were subjected to a maximum load repetition of 10,000 cycles. The results indicate that using three layers of geotextile beneath each course of the designed road pavement sections (surface, binder, and base) reduced rutting by 96%. Traffic benefit ratio (TBR) has been employed in this study to reveal the behavior of geotextile reinforcement in increasing the service life of the road. TBR values are the load cycling ratio between the reinforced and unreinforced section for the exact recorded rut depth, it has been found to be minimally equal to 4 for the case of using one layer of reinforcement at interface I, and that value keeps growing up for other reinforcement cases.

Keywords: geotextile reinforcement, road model, rutting, traffic benefit ratio (TBR)

1 Introduction

Stresses are the usual response of loading on flexible pavement and can be generated due to the effect of vehicular load on the pavement. The strain inside the layers of pavement is induced and begins to increase gradually as a result of the rapid growth in traffic, which leads to generating rutting stresses in the pavement. Shear deformation within the layers of flexible pavement contributes to the surface rutting of pavement. The plastic

*** Corresponding author: Tameem Mohammed Hashim,** Department of Building and Construction Techniques Engineering, Al-Mustaqbal University College, 51001 Hillah, Babylon, Iraq, e-mail: tameemmohammed@mustaqbal-college.edu.iq
Abdul Hadi Meteab AL Sa'adi: Department of Building and Construction Techniques Engineering, Al-Mustaqbal University College, 51001 Hillah, Babylon, Iraq, e-mail: abdulhadi.meteab@mustaqbal-college.edu.iq
Fatimah Fahem Al-Khafaji: Department of Architecture, Faculty of Engineering, University of Babylon, Hillah, Babylon, Iraq, e-mail: mat.fatimah.fahem@uobabylon.edu.iq
Munther Latif Abdul Hussein: Department of Building and Construction Techniques Engineering, Al-Mustaqbal University College, 51001 Hillah, Babylon, Iraq, e-mail: munther.latif@mustaqbal-college.edu.iq
Yasar Ameer Ali: Department of Building and Construction Techniques Engineering, Al-Mustaqbal University College, 51001 Hillah, Babylon, Iraq, e-mail: yessarameer@gmail.com
Alaa Hussein Ali: Department of Building and Construction Techniques Engineering, Al-Mustaqbal University College, 51001 Hillah, Babylon, Iraq, e-mail: alaahussein@mustaqbal-college.edu.iq
Yasir Mohammed Jebur: Department of Building and Construction Techniques Engineering, Al-Mustaqbal University College, 51001 Hillah, Babylon, Iraq, e-mail: yasir.mohammed@mustaqbal-college.edu.iq
Lina H. Ali: Department of Building and Construction Techniques Engineering, Al-Mustaqbal University College, 51001 Hillah, Babylon, Iraq, e-mail: lina.hussein@mustaqbal-college.edu.iq
Mohammed Zuhear Al-Mulali: Department of Building and Construction Techniques Engineering, Al-Mustaqbal University College, 51001 Hillah, Babylon, Iraq, e-mail: mohammed.zuhair@mustaqbal-college.edu.iq
Ashraf Anwer Al-Khazraji: Department of Building and Construction Techniques Engineering, Al-Mustaqbal University College, 51001 Hillah, Babylon, Iraq, e-mail: AshrafAlkhazraji@mustaqbal-college.edu.iq

deformation in the unbounded layers of pavement (subgrade, foundation, *etc.*) contributes to generating the rutting stresses [1]. Rutting of flexible pavement is also called wheel path, which is considered the most frequent defect in the pavement due to shear-strain deformations. These deformations are hard to determine and model due to variation in materials' characteristics and the permanent changes under the effect of load and temperature [2].

Geosynthetic reinforcement has proved to be a very supportive technique in road pavement by enhancing the bond between asphalt and aggregate and reducing the effect of shear deformation in subbase and subgrade courses. Also, using such reinforcement increases the stiffness of base course and bearing capacity of subgrade by minimizing normal stresses, prohibiting the local shear in subgrade and base, decreasing the influence of tension membrane and shear stresses of subgrade, and enhancing the distribution of loads on base layer [3].

Geosynthetic reinforcement can restrain the lateral movement of the subgrade and base layer and give support to the tensioned membrane where deep rutting occurs [4]. Meanwhile, an investigation of the behavior of asphalt pavement under the influence of reinforcement located at the bottom of the base course was carried out by Alimohammadi *et al.* [1].

Christopher has focused on examining the alterations in the characteristics of asphalt roads with the utilization of reinforcement within flexible pavement courses, between asphalt and aggregate layers, and the interface of any subsequent courses [5].

A few studies presented previously with a serious laboratory modeling, but all of these studies lack a full-scale model in the field; hence, this study aimed to simulate the true influence of truckload cycles and examine the behavior of asphalt pavement. The main issue of pavement in the southern and middle parts of Iraq is the permanent deformation, which is caused by the accumulation of load-induced deformation generated from all layers of pavement including the subgrade [6].

In this study the road model was built and constructed by using seven different positions of geosynthetic reinforcement, which is available locally. The research utilized one or more reinforcement sheets and recorded the behavior of the developed asphalt pavement in reducing the rutting failures.

2 Experimental works

2.1 Laboratory works

To evaluate the effects of using geotextile reinforcement on the pavement failures, caused by rutting, three types of pavement layers were selected (wearing, binder, and base courses). Therefore, three types of asphalt mixtures are prepared in the laboratory (control mixtures) using ordinary construction materials. A clear description of the used materials is shown below.

2.1.1 Asphalt binder

The used asphalt binder is (40–50) penetration grade brought from the AL-Nasseriya refinery. Table 1 presents the physical properties and tests of the asphalt binder.

2.1.2 Aggregate

The used course aggregate was crushed stones brought from the Al-Najaf quarry, which is widely utilized in the south and middle parts of Iraq in asphalt-paving projects. The aggregate particles are generally off-white with sharp surfaces.

Fine aggregate was also brought from the Al-Najaf quarry. The aggregate was then sieved and recombined to meet the Iraqi specifications (SCRB, R/9) for the wearing, binder, and base courses.

Table 2 presents the physical properties of the selected coarse and fine aggregate, whereas the selected gradation for the wearing, binder, and base courses are presented

Table 1: (40–50) Asphalt binder properties

Property	ASTM method	Unit	Test results	SCRB specification
Penetration at 25°C, 100 g, 5 s	D5	0.1 mm	46	40–50
Kinematic viscosity at 135°C	D2170	cst	383	—
Ductility at 25°C, 5 cm/min	D113–99	cm	138	>100
Flashpoint (Cleveland open cup)	D92	°C	256	Min. 232
Softening point	D36	°C	55	—
Specific gravity at 25°C	D70	—	1.03	—

Table 2: Aggregate's physical properties

Tests	ASTM code	Coarse aggregate wearing layer	Coarse aggregate binder layer	Coarse aggregate base layer	Fine aggregate
Apparent Specific gravity	C-127 C-128	2.551	2.556	2.650	2.54
Bulk specific Gravity	C-127 C-128	2.611	2.616	2.660	2.35
% water Absorption	C-127 C-128	0.83	0.9	1.42	2.8
Abrasion Los Angeles	C-131		25% (maximum 35%)		—
Angularity	D 5821		95%		—

Table 3: Aggregate gradation

Sieve size (mm)	Wearing layer		Binder layer		Base layer	
	Gradation	Limits	Gradation	Limits	Gradation	Limits
37.5					100	100
25			100	100	95	90–100
19	100	100	95	90–100	83	76–90
12.5	95	90–100	80	90–70	68	56–80
9.5	83	76–90	68	56–80	61	48–74
4.75	59	44–74	50	35–65	44	29–59
2.36	43	28–58	36	23–49	32	19–45
0.3	13	5–21	12	9–15	11	5–17
0.075	7	4–10	6	3–9	5	2–8

Table 4: Physical properties of filler

Tests	The result
Specific gravity (g/cm^2)	3.15
Fineness (cm^2/g)	3,046
% Passing sieve No. 200	96

in Table 3. The results of the tests indicated that the selected aggregates for the three layers met the Iraqi specifications (SCRB, R/9).

2.1.3 Mineral filler

Ordinary Portland cement was utilized as mineral fillers with the aid of its physical properties as shown in Table 4.

2.1.4 Geotextile reinforcement

The type of the used geotextile is a polypropylene biaxial geotextile, which is a polymeric-based, high-strength planar product. It has been utilized in the reinforcing actions of flexible pavement by confining the pavement structure and increasing its resistance to shear failures through the interlocking between the rectangular ribs and the asphaltic pavement. The primary goal of adopting geotextile materials is to improve performance while also saving money [7]. Physical properties of the used geotextiles as received from Sinan factory, Izmir, Turkey, are shown in Table 5. In addition, a tension test in (kN/m) has been performed on the geotextile using a microcomputer-controlled electronic universal machine connected to multiple ribs as shown in Figures 1–3 to predict the relationships of stress–strain and load–deformation of the used geotextile. Figure 4 represents a site photo of the used polypropylene biaxial geotextile.

Table 5: Physical properties of the used geotextile

Tests	Units	Long direction	Short direction
Unit weight	g/m^2	330	330
Aperture size	mm	34	24
Tensile strength at peak	kN/m	17	25
Tensile strength at 2% strain	kN/m	5	8
Yield point strain	%	9	8
Rib thickness	mm	1.1	1.54
Upper yield strength	MPa	3.1	1.03
Lower yield strength	MPa	3.1	1.03
Elastic modulus	GPa	0.98	0.58
Elongation of fracture percentage	%	−98	−98
Elongation percentage at maximum load	%	2.8	3.6
Total percentage of elongation	%	4.22	5

2.1.5 Indirect tensile strength test

The tensile strength of the generated asphaltic samples is found by the indirect tensile strength test, according to the method described in ASTM D 6931-07. Low-temperature cracking, fatigue, and rutting are the three major distress mechanisms. A higher tensile strength corresponds to a stronger cracking resistance. Specimens were prepared and left to cool at room temperature for 24 h and then put in a water bath at (20°C) for 30 min to evaluate the tensile strength resistance [8].

2.2 Field works

At the field, a temporary asphalt roadway was designed and constructed to enable the occurrence of rutting over the surface of the road, and that was achieved by:

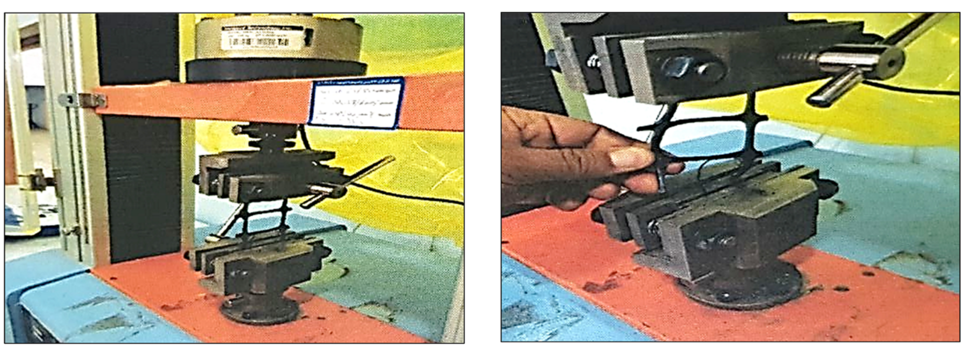

(a) (b)

Figure 1: Universal tensile testing machine. (a) Before the test and (b) after the test.

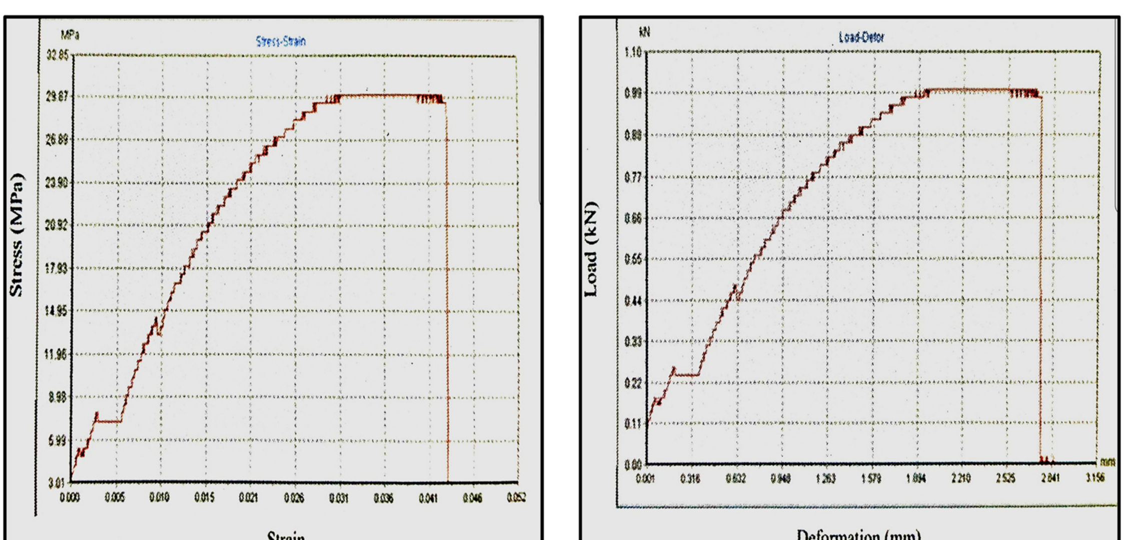

Figure 2: Stress–strain and load–deformation in the long direction.

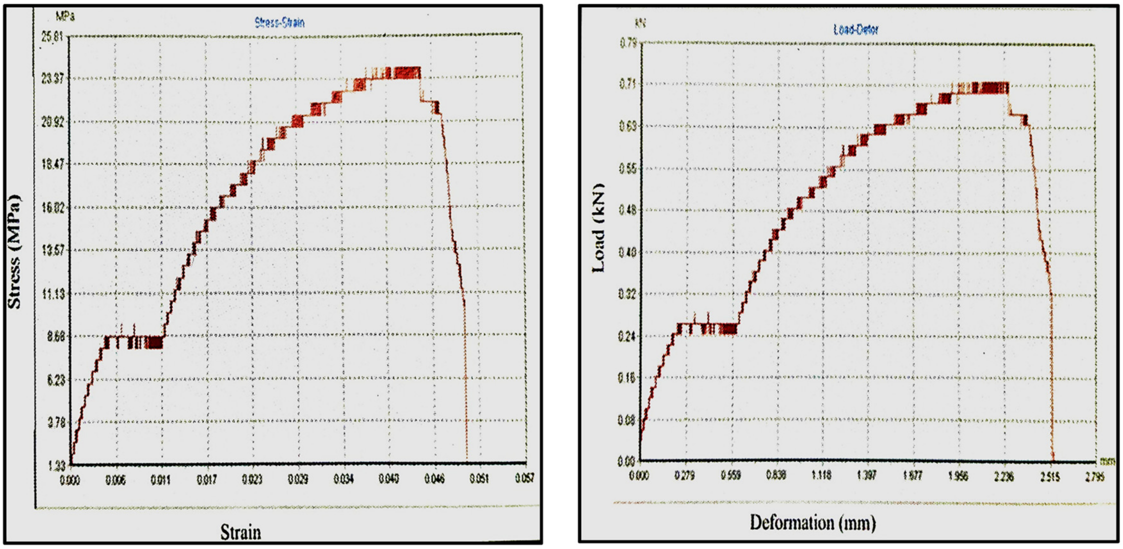

Figure 3: Stress–strain and load–deformation in the short direction.

Figure 4: Polypropylene biaxial geotextile.

- A field model was constructed using geotextile reinforcement and the tested construction materials as shown in Figure 5.
- Selecting seven different cases of reinforcement to have full comprehension of the flexible asphalt behavior under prospective dynamic axis loads was fixed in the interfaces I, II, and III as shown in Figures 6 and 7.

2.2.1 Constructing and testing the field model

Flexible pavement with a full scale was carried out carefully in the field with specific dimensions (28 m in length and 4.6 m in width). This model was trafficked to investigate the performance of each section (B–I) as shown in Figure 5 under the applied dynamic axial loads. All these sections were reinforced with geotextile layers in different positions. For example, zone B has a reinforcement placed in the interface between binder and wearing courses called (I), as shown in Figure 6, section B. The details of reinforcement for each section are shown in Figure 5 and detailed in Table 6.

The field model is connected with a 5 m unpaved section of road and a 1 m paved section to alleviate the negative influence of wheel torque, which results from the vehicular acceleration, and to facilitate the entrance and exit of vehicles.

In Figure 5, the end limps of the road are connected with two unpaved circular roads having a diameter of 22 m and super elevated to facilitate the rotation of vehicles with no acceleration or deceleration.

The truck is traveling (load cycling) for approximately 90 m to save a cycle time of 13 s (about 275 truck pass per hour), while the truck's average speed is 25 km/h. In June 2019, 10,000 truck cycles were achieved within 2 weeks. The selection of trafficking time depends on the highest temperature rate in Iraq, which is 43°C on average to examine the worst situation of rutting on road pavement [7].

Site preparation was achieved by involving cleaning issues, site leveling, grading by utilizing a lightweight grader, and fitting of geotextile in accordance with the design section of the model as shown in Figure 8 before conducting tests.

Manual spreading and overlapping (400 mm) were made to textile rolls (geo-synthetically the overlap was 300–450 mm in case the subgrade California bearing ratio (CBR) ≥ 2 and ≤ 4) [9]. Figure 8d shows the meshes

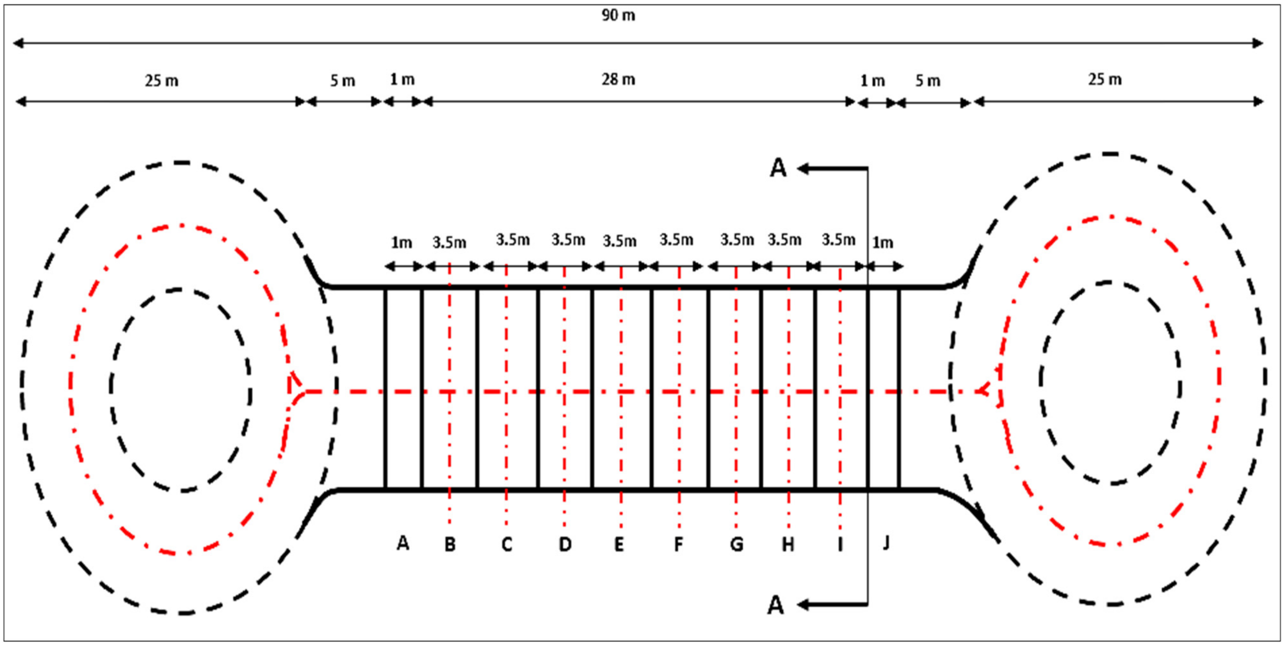

Figure 5: Full-scale road model.

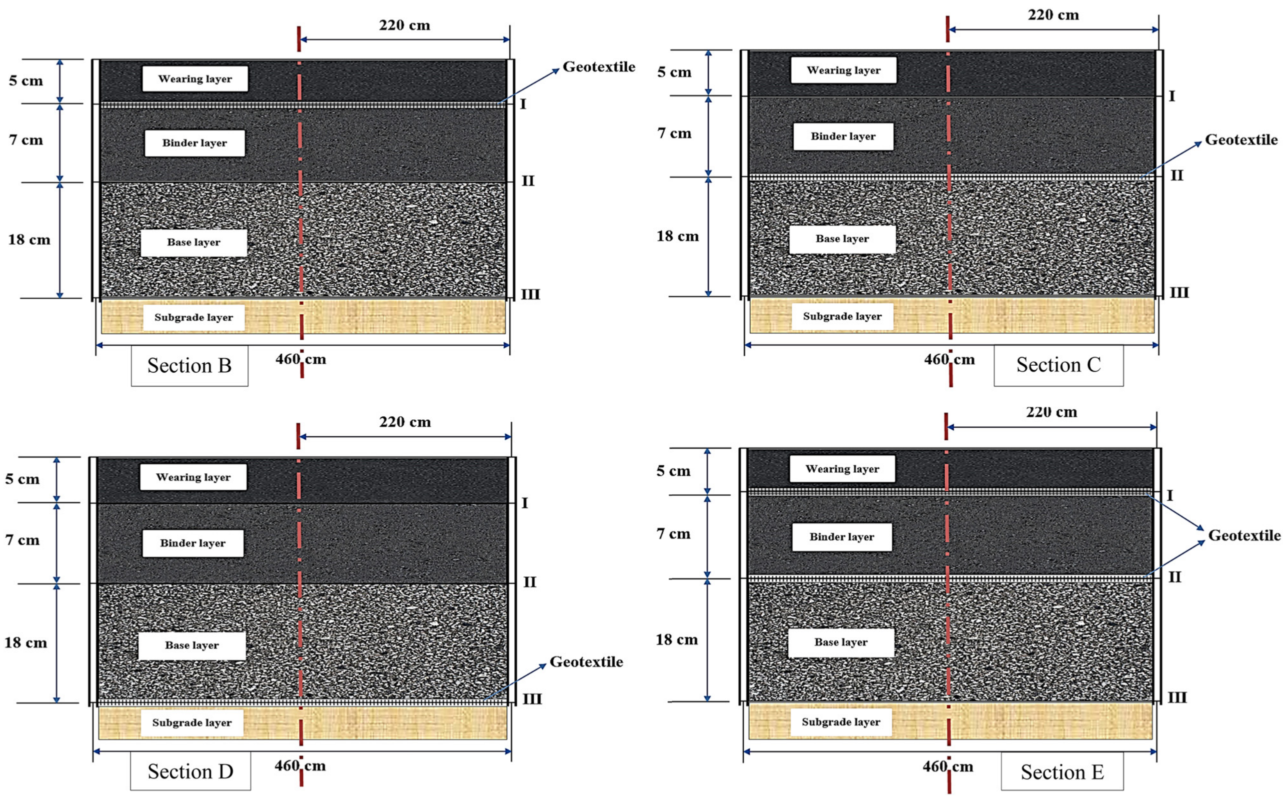

Figure 6: Sections B–E in the constructed road model.

of geotextile rolls fixed in contact with the surface of pavement course by hilted screws for paved roads and anchored pins for soil surface at a rate of 2 per m^2.

Spreading of prime coat at interface II and tack coat at the interface I is in accordance with Iraqi specifications [10]. After placing the geotextile mesh, tack and prime

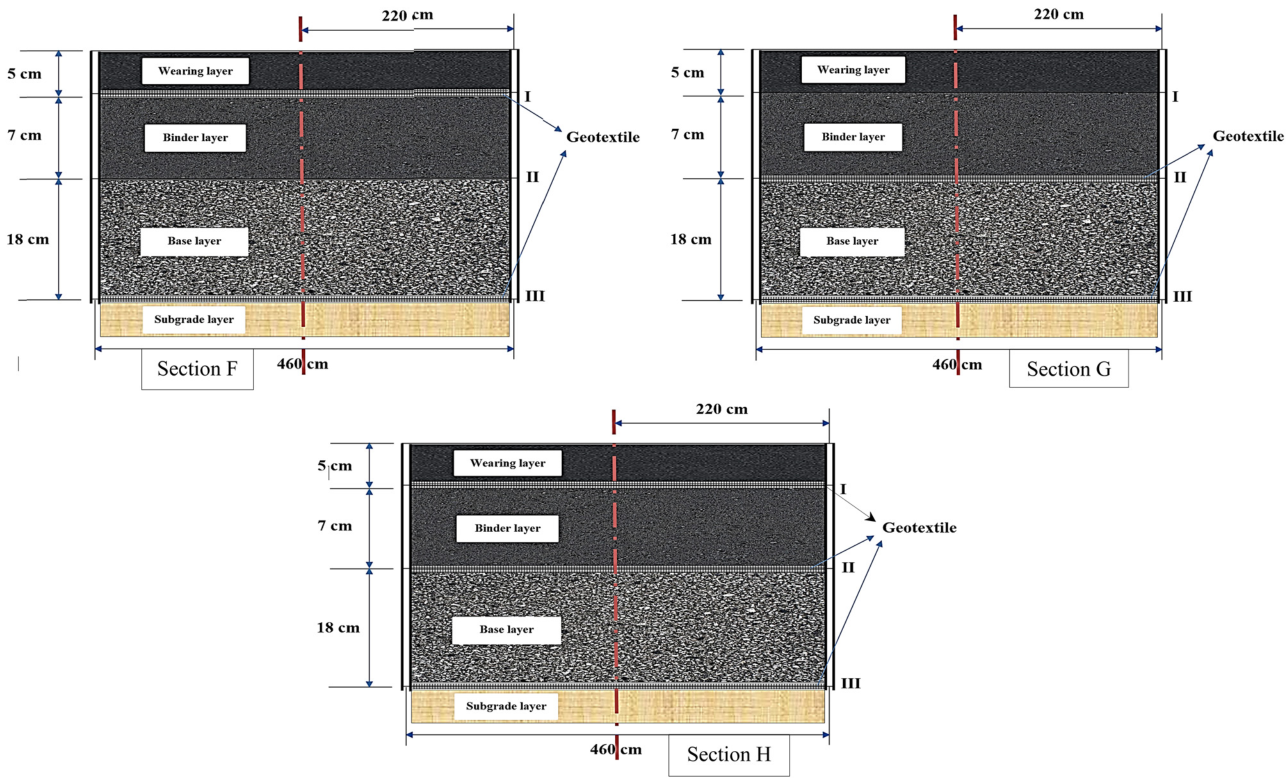

Figure 7: Sections F–H in the constructed road model.

Table 6: Model sections reinforcement designation

Section	Designation of reinforcement	Locations
A	—	Entrance and exit areas
B	I	Reinforcement is in the interface between binders and wearing courses
C	II	Reinforcement is in the interface between base and binder courses
D	III	Reinforcement is in the interface between subgrade and base courses
E	I + II	Ubiquitously utilization for reinforcement in sections I and II
F	I + III	Ubiquitously utilization for reinforcement in sections I and III
G	II + III	Ubiquitously utilization for reinforcement in sections I and II
H	I + II + III	Ubiquitously utilization for reinforcement in sections I, II, and III
I	With no reinforcement	No reinforcement (control section)
J	—	Entrance and exit areas

coats are incorporated to enhance the bonding of surfaces being in contact. By using the spreading machine, wearing materials and a bituminous binder are supplied and spread. The properties of the constructed model were compared with Iraqi standards [10].

2.2.2 The applied loads on the field model

Tandem axles were chosen for the loading process on the road model, which consists of a single tire front axle and dual tire rear axle. An overload of 49 and 98 kN at the rear axle of the truck was used to create a loading condition with a magnitude of 24.5 kN in each wheel. The pressure in each tire size is 830 kPa (120 psi).

2.2.3 Rutting measurement of the field model

During trafficking, traverse measurements of up-lift and down-lift ruts were taken every 1,000 cycles using a 100 mm dial gauge sensitive to 0.1 mm. An extension

Figure 8: Site preparation. (a) High plasticity subgrade, (b) wearing layer layout, (c) rigid iron beam, and (d) geotextile roll.

part of 76 mm was added to this gauge to get the rutting reading in the control section (without reinforcement).

A rigid iron beam with uniform steady support for the dial indicator is installed to gain high-accuracy results. The attached support to the iron beam can be easily fixed for each 100 mm as shown in Figure 8c. Both sides of the rigid beam consist of two limited, stable, and leveled legs placed at the end of the sections. The dial recorded the first reading in the centerline of the road and the second reading for the left and right sides of the road.

2.3 Full-scale road construction and stratification

To facilitate the testing mechanism, an asphalt roadway section has been designed with light traffic loading as shown in Figures 5, 8a and b. The layers of the road cross-section are:

- Wearing course made of asphalt, 50 mm in thickness and 12.5 mm nominal aggregate size;
- Binder course made of asphalt, 70 mm in thickness and 19 mm nominal aggregate size; and
- Base course made of sand mix and gravel, 180 mm in thickness and 37.5 mm nominal aggregate size.

The layer geotextile of 24 mm was used across vehicle direction while the layer of 34 mm was used in vehicle direction as a reinforcement layer. CBR test was conducted in the field for subgrade soil in accordance with ASTM D1883-16 and found to be 3% [11]. In addition, the water content was 18%, the liquid limit was 48%, and the plastic index was 22% in accordance with Iraqi specifications (SCRB, R/9).

3 Results and discussion

Laboratory results for the Marshall volumetric properties (ASTM D6927-06) of the control mixture (without geotextile reinforcement as shown in Figure 10) are tabulated in Table 7 and Figure 9. Also, the results of the indirect tensile strength test are shown in Figure 11.

The results of the field rutting for road sections with and without reinforcement are shown in Figures 12–19. Seven different positions of the geotextile reinforcement are used within the model of flexible pavement to

Table 7: Marshall volumetric properties

Property	Wearing layer	S.C.R.B. standards	Binder layer	S.C.R.B. standards	Base layer	S.C.R.B. standards
Stability (kN)	11.2	Min. 8	10.35	Min. 7	9.65	Min. 5
Flow (mm)	3.75	2–4	3.0	2–4	2.5	2–4
Bulk density (g/cm^3)	2.361	—	2.354	—	2.321	—
Air voids %	4.0	3–5	4.0	3–5	4.0	3–6
O.A.C. %	4.9	4–6	4.6	4–6	4.1	3–5.5

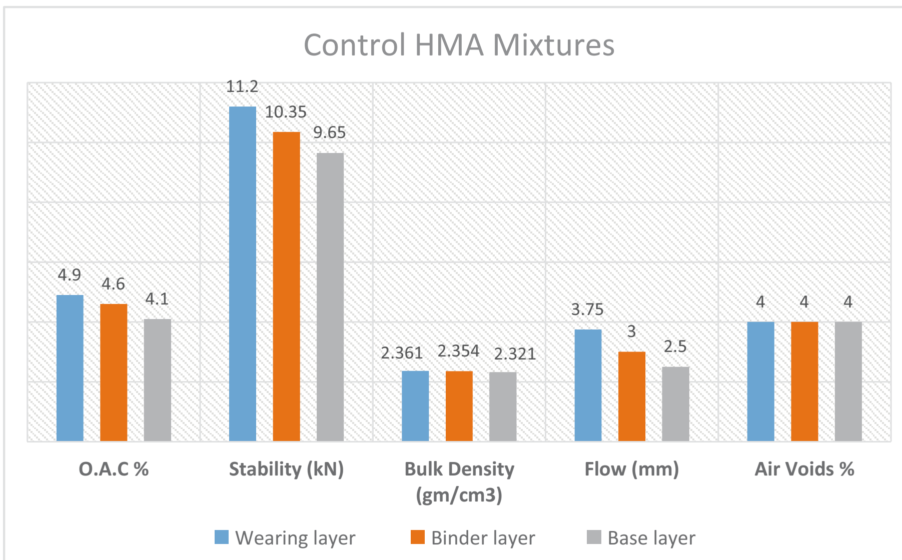

Figure 9: Comparison of Marshall properties between the selected layers.

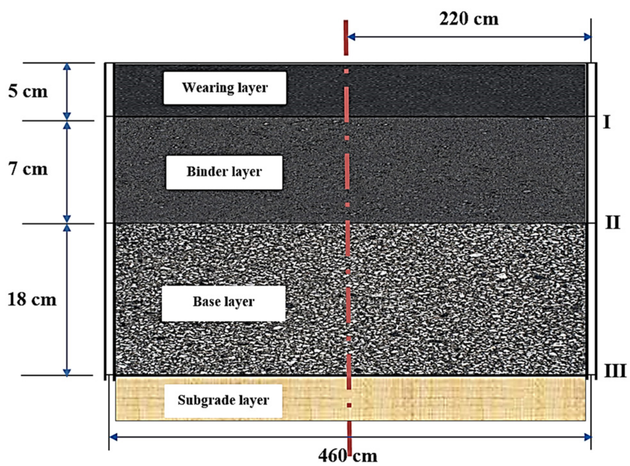

Figure 10: The control section A–A in the road model.

demonstrate the effect of reinforcement on the rutting values and compare the results with the control section (no reinforcement). The mentioned figures are showing the variations in shape, rut area, and behavior of sections under variable load cycle. The values of down-left, up-lift, and total ruts are presented graphically in Figures 20 and 21. In addition, the same figures demonstrate the increase in rutting values under load cycle repetition (N).

Correlations between rut depth and various numbers and positions of geotextile reinforcement are shown in Figure 20, whereas for 10,000 load cycles, the curve shows a significant decrease in rut depth when one or more reinforcement layer is utilized. In addition, the location of the reinforcement within pavement layers has a significant role in decreasing the rutting values and that leads to an increase in the service life of the road. Figures 20 and 21 prove that putting one layer of geotextile reinforcement at interface II has enhanced the performance of the road while putting the same layer at interface III has also enhanced the road performance but in a way

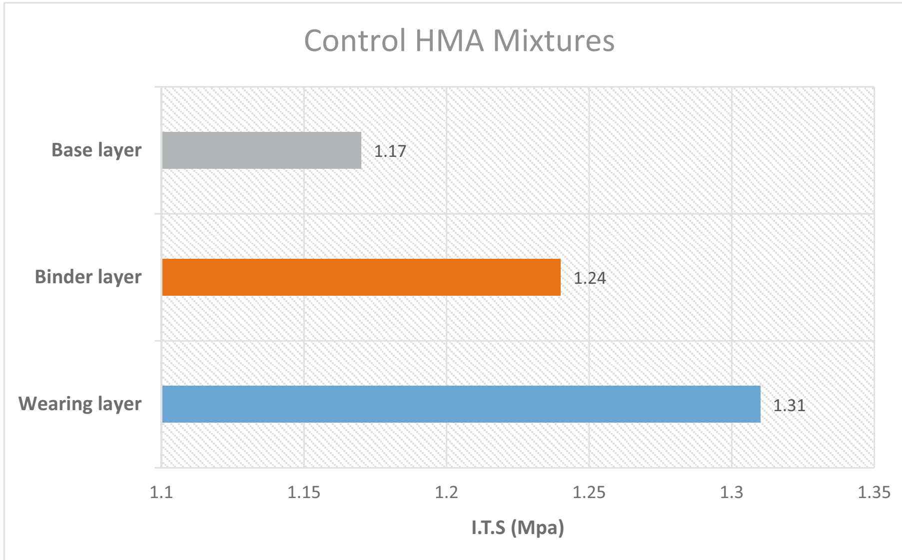

Figure 11: The results of the I.T.S. test for the selected layers.

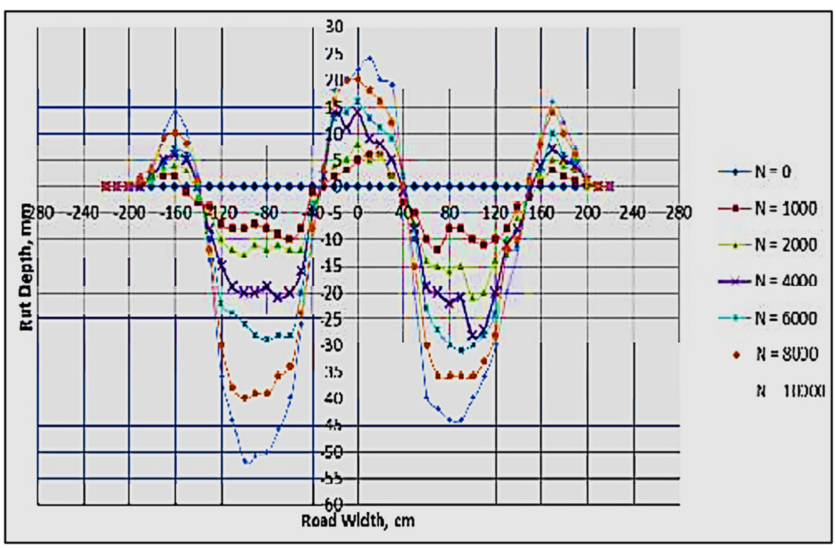

Figure 12: Rutting depth at interface I.

lesser than the first position. Regarding the effects of reinforcement the influence of reinforcement on minimizing the rutting values is significantly low when placed at the interface I, in comparison with that gained when placing reinforcement at interfaces II and III, which can be explained owing to putting reinforcement at the interface I give lateral resistance as a result to the forces of friction and interlocking between the bottom of wearing layer and geotextile. This position of reinforcement reduces the physical activity of the geotextile sheet, fortunately, that leads to an increase in the membrane support of wheel loads and the bearing capacity of failure zones within the considered pavement layers to enhance the shear strength of the interface I [12].

Using two layers of reinforcement in three various locations at I + II, I + III, and II + III or three layers of reinforcement as shown in Figures 20 and 21 indicated that understanding the pavement behavior is very complex and that is mainly owing to the accumulated enhancement, which occurs as a result of placing three layers of reinforcement in the selected interfaces.

By employing the traffic benefit ratio (TBR = NR/Nu) in which Nu is the number of load cycles for the unreinforced section and NR is the number of load cycles in the

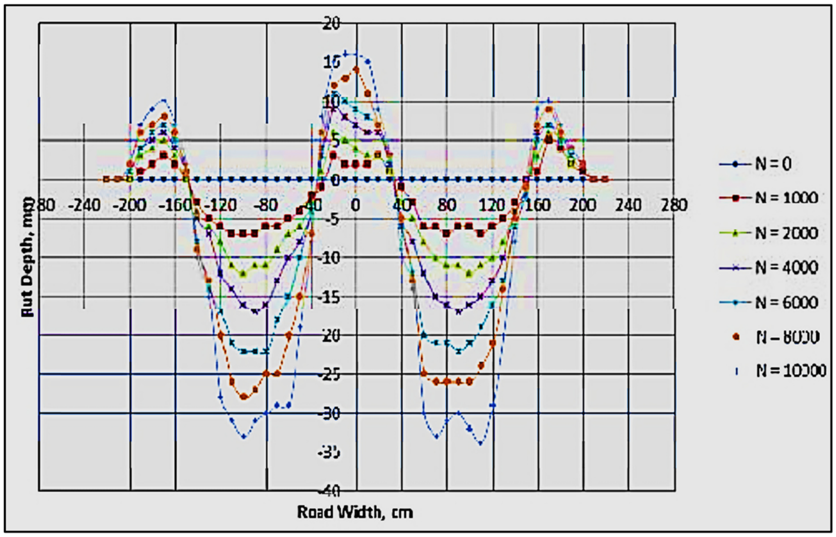

Figure 13: Rutting depth at interface II.

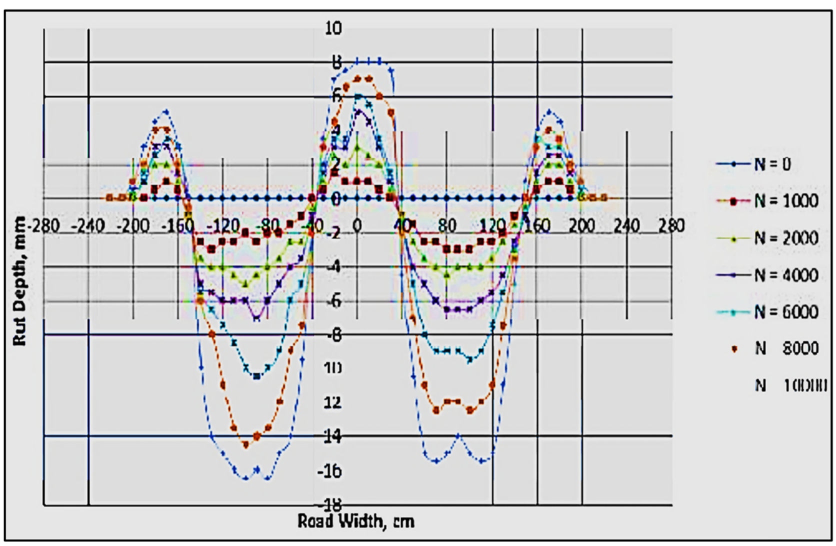

Figure 14: Rutting depth at interface III.

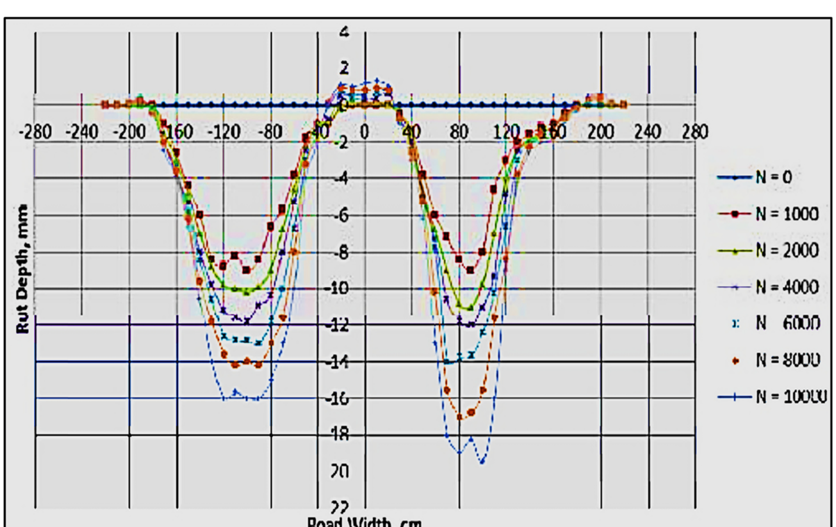

Figure 15: Rutting depth at interfaces I + II.

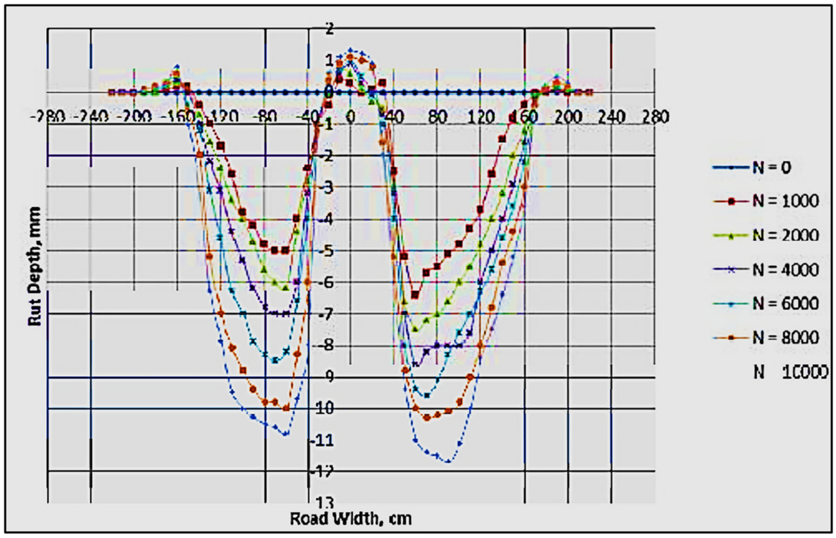

Figure 16: Rutting depth at interfaces I + III.

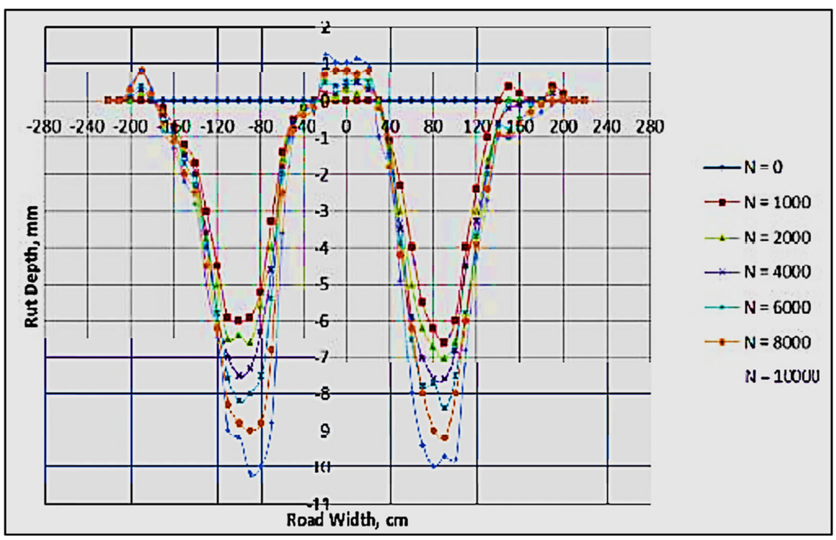

Figure 17: Rutting depth at interfaces II + III.

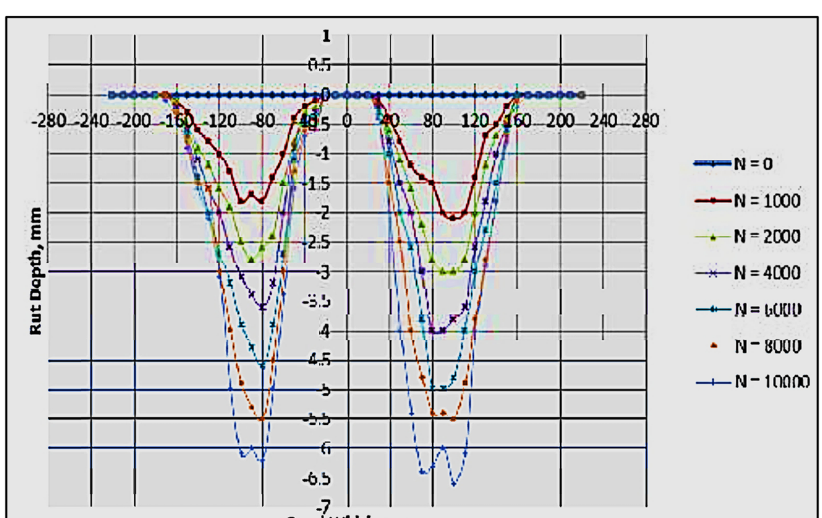

Figure 18: Rutting depth at interfaces I + II + III.

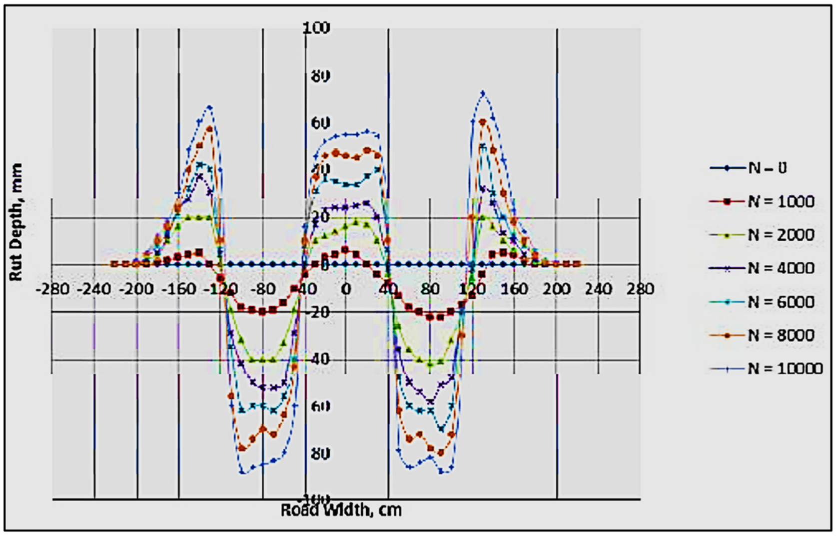

Figure 19: Rutting at the control section.

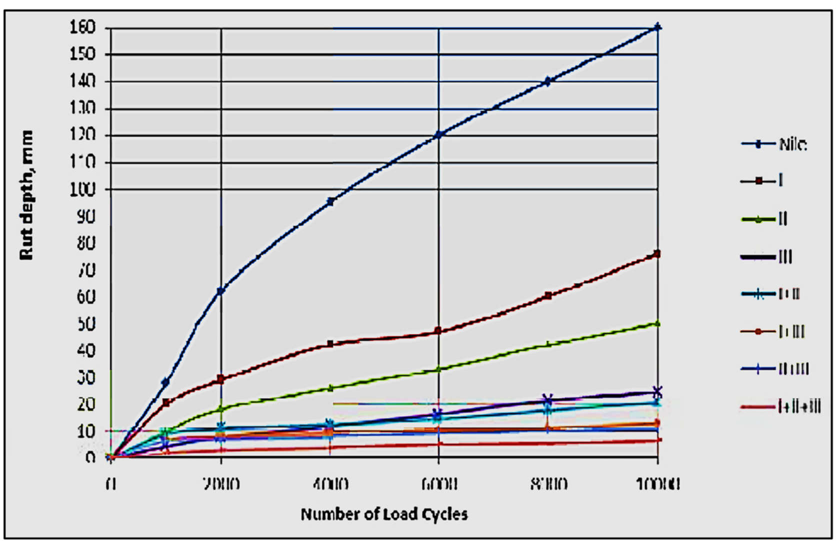

Figure 20: Rutting depth at different load cycles and interfaces.

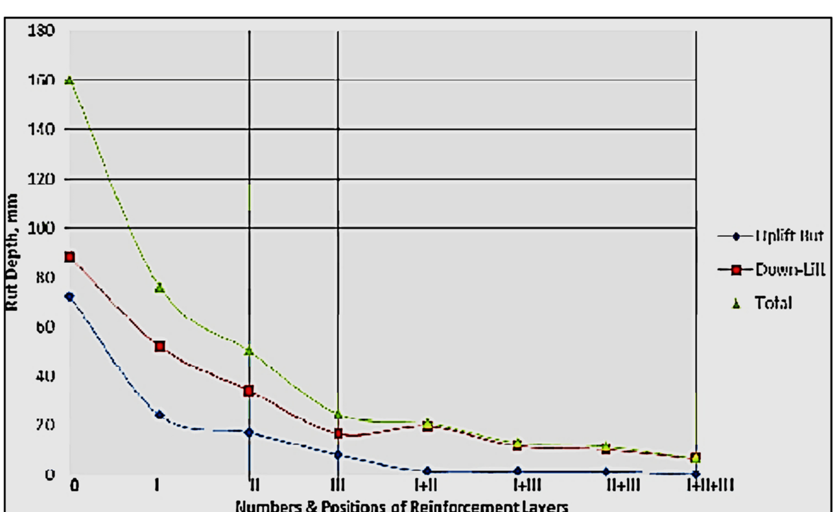

Figure 21: Rutting depth at different numbers and positions of reinforcement layers under 10,000 load cycles.

reinforced section [11]. At interfaces I and II, TBR values are equal to 4 and 6.3, respectively, whereas the rut depth is 45 mm as shown in Figure 20. TBR values were significantly high in other reinforcement cases, whereas these values indicated the behavior of geotextile reinforcement in increasing the service life of the road [13].

4 Conclusions and recommendations

In this study, the following conclusions can be drawn:

- The paved roads that are reinforced with multi-geotextile layers offer less rutting than the singly reinforced.
- Rutting depth decreases by 96% with the use of triple layers of reinforcement as in interfaces (I + II + III).
- Regarding the singly reinforced layers, interface III is the best case of reinforcement because the developed rutting has been reduced by 85%.
- Regarding the doubly reinforced layers, interfaces II + III are the best case of reinforcement since the reduction in rutting reaches 93% in comparison to the control section (without reinforcement).
- In the case of triply reinforced layers, interfaces I + II + III are the best case of reinforcement owing to the reduction in rutting to 96% by comparing it with the control section (without reinforcement).
- A considerable increase in TBR that occurs at interfaces I and II reaches 4 and 6.3, respectively, by using one layer of reinforcement, which is corresponding to 45 mm rut depth. This is due to the increase in the road service life by 4 times at interface I and 6.3 times at interface II when the other circumstances are the same.

To reduce the permanent deformations of rutting, it is recommended to use the geotextile reinforcing technique in constructing the layers of flexible pavement, especially in the high-temperature regions in Iraq. In addition, using such a method leads to minimizing the maintenance processes of the flexible pavement.

Funding information: The authors state no funding involved.

Author contributions: All authors have accepted responsibility for the entire content of this manuscript and approved its submission.

Conflict of interest: The authors state no conflict of interest.

References

[1] Alimohammadi H, Schaefer VR, Zheng J, Li H. Performance evaluation of geosynthetic reinforced flexible pavement: a review of full-scale field studies. Int J Pavement Res Technol. 2020 Jul 2;14(1):30–42.
[2] Zhao Y, Zhou S, Zhao C, Valeo C. The influence of geotextile type and position in a porous asphalt pavement system on Pb (II) removal from stormwater. Water. 2018;10(9):1205.
[3] Saghebfar M, Hossain M, Lacina BA. Performance of geotextile-reinforced bases for paved roads. Transport Res Rec. 2016;2580(1):27–33.
[4] Kermani B, Xiao M, Stoffels SM, Qiu T. Reduction of subgrade fines migration into subbase of flexible pavement using geotextile. Geotext Geomembr. 2018;46(4):377–83.
[5] Christopher BR. Cost savings by using geosynthetics in the construction of civil works projects. Proceedings of the 10th International Conference on Geosynthetics; Berlin, Germany; 2014 Sep 21.
[6] Anusudha V, Sunitha V, Babu C, Bhole CR, Mathew S. Numerical studies on coir geotextile reinforced flexible pavement. Lecture Notes Civ Eng. 2020;76:627–36.
[7] Ullah S, Tanyu BF, Guler EF, Hoppe EJ, Akmaz E. Evaluation of the long-term performance of woven geotextile used between base course and subgrade of a paved road. Transport Res Rec. 2019;2673(8):310–21.
[8] ASTM D6931-07. Standard Test Method for Indirect Tensile (IDT) Strength of Bituminous Mixtures. ASTM International. West Conshohocken, PA: 2016. p. 19428–2959.
[9] Kumar PS, Rajkumar R. Effect of geotextile on CBR strength of unpaved road with soft subgrade. Electron J Geotech Eng. 2012;17(1):1355–63.
[10] State Corporation for Roads and Bridges. General Specification for Roads and Bridges (SORB/R9)—Hot Mix Asphaltic Concrete Pavement. Republic of Iraq, Ministry of Housing and Construction; 2003.
[11] ASTM D1883-16. Standard test method for california bearing ratio (CBR) of laboratory-compacted soils. West Conshohocken, PA: ASTM International; 2016.
[12] Kinney TC, Abbott J, Schuler J. Benefits of using geogrids for base reinforcement with regard to rutting. Transport Res Rec. 1998;1611:86–96.
[13] Imjai T, Pilakoutas K, Guadagnini M. Performance of geosynthetic-reinforced flexible pavements in full-scale field trials. Geotext Geomembr. 2019 Apr 1;47(2):217–29.